INTERNATIONAL JOURNAL OF CHEMICAL REACTOR ENGINEERING

Volume 5 2007 *Article* A35

Hydrodynamic and Thermal Modelling of Gas–Particle Flow in Fluidized Beds

O. S. Abd El Kawi* E. F. Atwan† S. A. Abdelmonem‡

A. M. Abdalla** K. M. Elshazly††

*Nuclear Research Center, Atomic Energy Authority, usama_ali35@hotmail.com

†Benha University, efatwan@yahoo.com

‡Benha University, s_moniem@yahoo.com

**Nuclear Research Center, Atomic Energy Authority, usama1_ali35@hotmail.com

††Benha University, kmshasan@link.net

ISSN 1542-6580

Hydrodynamic and Thermal Modelling of Gas–Particle Flow in Fluidized Beds

O. S. Abd El Kawi, E. F. Atwan, S. A. Abdelmonem, A. M. Abdalla, and K. M.Elshazly

Abstract

In this study a mathematical model has been developed to simulate two dimensional fluidized beds with uniform fluidization. The model consists of two sub models for hydrodynamic and thermal behavior of fluidized beds on which a FORTRAN program entitled (NEWFLUIDIZED) is devolved .The program is used to predict the volume fraction of gas and particle phases, the velocity of the two phases, the gas pressure and the temperature distribution for two phases. Also the program calculates the heat transfer coefficient. Besides that, the program predicts the fluidized bed stability and determines the optimum input gas velocity for fluidized beds to achieve the best thermal behavior. The hydrodynamic model is verified by comparing its results with the computational fluid dynamic code MFIX [1]. The thermal model was tested and compared to the available previous experimental correlations. The model results show good agreement with MFIX results and the thermal model of the present work confirms Zenz [2] and Gunn [3] equations.

KEYWORDS: fluidization, hydrodynamic, Eulerian–Eulerian model

1. INTRODUCTION

Fluidization refers to the contact between a bed of solids and a flow of fluid. As a result, the solid particles are transformed into fluid like state through suspension in a gas or liquid. Liquid–solid systems exhibit particulate fluidization, which results in a stable homogenous bed, with especially uniform distribution of solids. Gas-solid systems, generally, exhibit an aggregative behavior completely different from that of liquid – solid systems. Here the beds are no longer homogenous and have important void volumes. The system of interest in this study is gas-solid fluidization, which refers to the contacting of solid materials with gas. As the gas flows through the material. A two-phase mixture with some unique characteristics is formed. The solids expand and flow with the gas depending on the physical conditions of the solids and on the gas velocity [4].The widespread applications of fluidized beds in industry and the demand for improvements in fluidization efficiency have increased the need for accurate fluidization modelling. Although this poses a considerable challenge, due to the complexity of fluidization physics. Computer hardware development and advances in numerical methods are now providing the necessary means to investigate the validity of several modelling approaches. By comparing numerical simulations with experiments, these modelling approaches can be validated and used with confidence to aid design and operation of fluidized beds [5].Computational fluid dynamic models for gas–solid flow can be divided into two groups, the Lagrangian-Eulerian models and the Eulerian–Eulerian models. The Lagrangian approach describes the solid phase at a particle level and the gas phase as a continuum. On the other hand The Eulerian–Eluerian approach is based on the two fluid model (TFM) that treats each phase as an interpenetrating continuum. The TFM is perhaps the most commonly used model for predicting the dynamic behaviour of fluid particle systems [6]. In the present work the Eulerian-Eulerian method has been used, where a mathematical modelling and numerical simulation of the hydrodynamics and heat transfer processes in a two dimensional gas fluidized bed with a vertical uniform gas velocity at the inlet have been created. The velocity, volume fraction, temperature distribution for gas phase and particle phase are calculated. Also gas pressure and average heat transfer coefficient prediction will be studied as well. The model is validated and verified by the experimental and numerical data. A computational fluid dynamic code called “MFIX” is used to validate the present work hydrodynamic model. Such a simulation technique allows performance evaluation for different bed input parameters, and can evolve into a tool that would help in the optimum design of fluidized for different industrial use.

2. MATHEMATICAL MODEL

A hydrodynamic and thermal model for the fluidized bed is developed based on schematic diagram shown in Figure (1). The principles of conservation of mass, momentum and energy are used in the present hydrodynamic and thermal models of fluidized bed. The bed is 2-dimensional filled with particles with the same diameters dp. Uniform fluidization and constant input fluid flux are assumed. Both particle and gas have constant density and gas has constant viscosity .It is assumed that there is no chemical reaction or mass transfer between gas and solid. The expanded bed region is considered in the analysis in addition to the out flowing gas. Viscous heating effects are neglected.

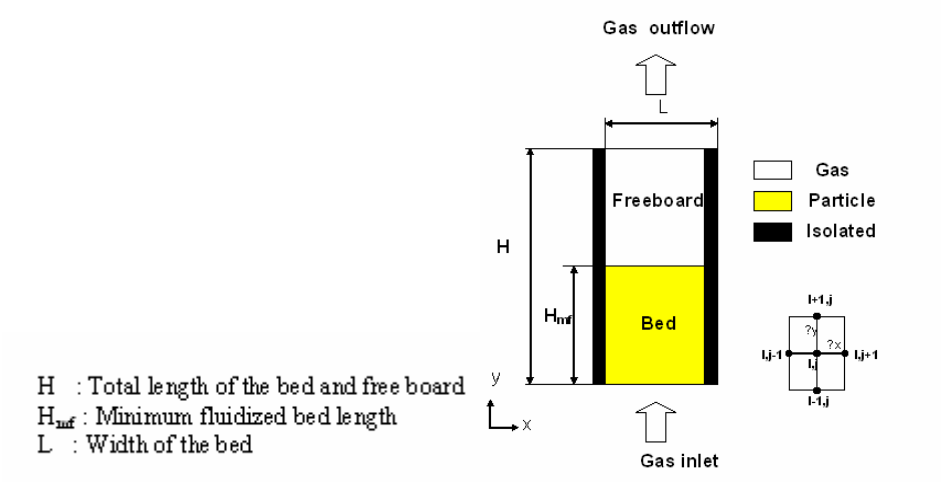

Figure (1): Present work schematic diagram

2.1 Governing Equations

Eulerian-Eulerian approach was applied in the present work model. For the gas phase, the equations of conservation of mass, momentum and energy are written as following [7] :

Gas phase continuity,

$$\frac{\partial \varepsilon_g}{\partial t} + \frac{\partial}{\partial x}(\varepsilon_g u_g) + \frac{\partial}{\partial y}(\varepsilon_g v_g) = 0 \tag{1}$$

Gas phase momentum,
"x -direction "

$$\rho_g \varepsilon_g \frac{\partial u_g}{\partial t} + \rho_g \varepsilon_g \frac{\partial}{\partial x}(u_g u_g) + \rho_g \varepsilon_g \frac{\partial}{\partial y}(v_g u_g) = F_{gx} \tag{2}$$

"y -direction "

$$\rho_g \varepsilon_g \frac{\partial v_g}{\partial t} + \rho_g \varepsilon_g \frac{\partial}{\partial x}(u_g v_g) + \rho_g \varepsilon_g \frac{\partial}{\partial y}(v_g v_g) = F_{gy} \tag{3}$$

where,

$$F_{gy} = -C_d \frac{3\varepsilon_s \rho_g (v_g - v_s)|v_g - v_s|}{4 d_p}(1-\varepsilon_s)^{-1.8} - \varepsilon_g \rho_g g - \varepsilon_g \frac{\partial p}{\partial y} \tag{4}$$

$$F_{gx} = -F_{sx} = -C_d \frac{3\varepsilon_s \rho_g (u_g - u_s)|u_g - u_s|}{4 d_p}(1-\varepsilon_s)^{-1.8} + \varepsilon_s \frac{\partial p}{\partial x} \tag{5}$$

Gas phase energy equation [8]:

$$\rho_g C_{pg} \frac{\partial \varepsilon_g T_g}{\partial t} + \rho_g C_{pg} \frac{\partial}{\partial x}(\varepsilon_g u_g T_g) + \rho_g C_{pg} \frac{\partial}{\partial y}(\varepsilon_g v_g T_g) = \frac{\partial}{\partial x}(\varepsilon_g k_g \frac{\partial T_g}{\partial x})$$
$$+ \frac{\partial}{\partial y}(\varepsilon_g k_g \frac{\partial T_g}{\partial y}) + h_v (T_s - T_g) \tag{6}$$

Also the conservation equations for the particle phase are as following:
Particle phase continuity

$$\frac{\partial \varepsilon_s}{\partial t} + \frac{\partial}{\partial x}(\varepsilon_s u_s) + \frac{\partial}{\partial y}(\varepsilon_s v_s) = 0 \tag{7}$$

Particle phase momentum
"x -direction "

$$\rho_s \varepsilon_s \frac{\partial u_s}{\partial t} + \rho_s \varepsilon_s \frac{\partial}{\partial x}(u_s u_s) + \rho_s \varepsilon_s \frac{\partial}{\partial y}(v_s u_s) = F_{sx} \tag{8}$$

"y -direction "

$$\rho_s \varepsilon_s \frac{\partial v_s}{\partial t} + \rho_s \varepsilon_s \frac{\partial}{\partial x}(u_s v_s) + \rho_s \varepsilon_s \frac{\partial}{\partial y}(v_s v_s) = F_{sy} \tag{9}$$

where ,

$$F_{sy} = C_d \frac{3\varepsilon_s \rho_g (v_g - v_s)|v_g - v_s|}{4d_p}(1-\varepsilon_s)^{-1.8} - \varepsilon_s \rho_s g - \varepsilon_s \frac{\partial p}{\partial y} - \frac{\partial \varepsilon_s}{\partial y}(3.2 g d_p \varepsilon_s (\rho_s - \rho_g)) \tag{10}$$

$$F_{sx} = C_d \frac{3\varepsilon_s \rho_g (u_g - u_s)|u_g - u_s|}{4d_p}(1-\varepsilon_s)^{-1.8} - \varepsilon_s \frac{\partial p}{\partial x} \tag{11}$$

Particle phase energy Equation [8] :

$$\rho_s C_{ps} \frac{\partial \varepsilon_s T_s}{\partial t} + \rho_s C_{ps} \frac{\partial}{\partial x}(\varepsilon_s u_s T_s) + \rho_s C_{ps} \frac{\partial}{\partial y}(\varepsilon_s v_s T_s) = \frac{\partial}{\partial x}(\varepsilon_s k_s \frac{\partial T_s}{\partial x})$$
$$+ \frac{\partial}{\partial y}(\varepsilon_s k_s \frac{\partial T_s}{\partial y}) + h_v (T_g - T_s) + \varepsilon_s \dot{q} \tag{12}$$

2.2 Constitutive Equations

To close the above equations set constitutive equations that are required for continuity, momentum and energy equations. These constitutive equations are listed as following:

Volume Fraction Constraint

$$\varepsilon_g + \varepsilon_s = 1.0 \tag{13}$$

Relation between Fluid and Particle Velocities [7]

$$V_{gin} = \varepsilon_g v_g + \varepsilon_s v_s \tag{14}$$

$$U_{gin} = \varepsilon_g u_g + \varepsilon_s u_s \tag{15}$$

Combined Momentum Equations [7]:
x- direction:

$$\rho_s \left[\frac{\partial u_s}{\partial t} + \frac{\partial}{\partial x}(u_s u_s) + \frac{\partial}{\partial y}(v_s u_s) \right] + \rho_g \left[\frac{\partial u_s}{\partial t} + \frac{\partial}{\partial x}(u_g u_g) + \frac{\partial}{\partial y}(v_g u_g) \right] = 0 \tag{16}$$

y- direction:

$$\rho_s \left[\frac{\partial v_s}{\partial t} + \frac{\partial}{\partial x}(u_s v_s) + \frac{\partial}{\partial y}(v_s v_s) \right] - \rho_g \left[\frac{\partial v_g}{\partial t} + \frac{\partial}{\partial x}(u_g v_g) + \frac{\partial}{\partial y}(v_g v_g) \right] = \frac{F_{sy}}{\varepsilon_s} - \frac{F_{gy}}{\varepsilon_g} \tag{17}$$

Drag Coefficient

$$C_d = \left(0.63 + \frac{4.8}{\mathrm{Re}^{0.5}} \right)^2 \tag{18}$$

with particle Reynolds number :

$$\mathrm{Re} = \frac{\varepsilon_g \rho_g d_p |\overrightarrow{U_r}|}{\mu_g} \tag{19}$$

Gas Pressure Drop [7] :

$$P_{g,in} = P_{g,out} + \rho_g g\left(H - H_{mf}\right) + \left(\rho_g \varepsilon_{g,mf} + \rho_s\left(1 - \varepsilon_{g,mf}\right)\right) g H_{mf} \tag{20}$$

$$\rho_{sus} = \rho_s \varepsilon_s + \rho_g \varepsilon_g \tag{21}$$

$$\Delta P_g = \rho_{sus} g h \tag{22}$$

Thermal Conductivity Values (k_g and k_s) [9]:

$$k_{bg} = \left(1 - \sqrt{1 - \varepsilon_g}\right) k_{go} \tag{23}$$

$$k_{bs} = \sqrt{1 - \varepsilon_g}\left(\omega A + (1 - \omega)\Gamma\right) k_{go} \tag{24}$$

$$\Gamma = \frac{2}{\left(1 - \frac{B}{A}\right)}\left[\frac{A-1}{\left(1 - \frac{B}{A}\right)^2}\frac{B}{A} Ln\left(\frac{A}{B}\right) - \frac{B-1}{\left(1 - \frac{B}{A}\right)} - \frac{1}{2}(B+1)\right] \tag{25}$$

$$B = 1.25\left(\frac{1 - \varepsilon_g}{\varepsilon_g}\right)^{\frac{10}{9}} \tag{26}$$

$$A = \frac{k_{s,o}}{k_{g,o}} \tag{27}$$

$$\omega = 7.26 X 10^{-3} \tag{28}$$

$$k_g = \frac{k_{b,g}}{\varepsilon_g} \tag{29}$$

$$k_s = \frac{k_{b,s}}{\varepsilon_s} \tag{30}$$

Interphase volumetric Heat Transfer coefficient h_v [3]:

$$Nu = \frac{h_{gp} d_p}{k_{g,o}} \tag{31}$$

$$Nu = \left(7 - 10\varepsilon_g + 5\varepsilon_g^2\right)\left(1 + 0.7\,\mathrm{Re}_p^{0.2}\,\mathrm{Pr}^{\frac{1}{3}}\right) + \left(1.33 - 2.40\varepsilon_g + 1.20\varepsilon_g^2\right)\mathrm{Re}_p^{0.7}\,\mathrm{Pr}^{\frac{1}{3}} \tag{32}$$

$$\mathrm{Pr} = \frac{C_{p,g}\mu_g}{k_{g,o}} \tag{33}$$

$$h_v = \frac{6\left(1 - \varepsilon_g\right) h_{gp}}{d_p} \tag{34}$$

2.3 Boundary and Initial Conditions

The system of conservation equations (1),(2),(3),(6),(7),(8),(9),(12),and(13),nine equations which discuss in previous sections must be solved for the nine dependent variables: the gas-phase volume fraction ε_g, the particle-

phase volume fraction ε_s , the gas pressure P_g, the gas velocity components u_g and v_g and the solids velocity components u_s and v_s in the *x*- and *y*- directions, respectively ,the gas temperature T_g and particle temperature T_s. To avoid the numerical instability problems due to the fluctuation in gas pressure the combined momentum equations is used. The combined momentum equation is produced by combining the fluid and particle momentum equations (3),(4),(5) and (6) by elimination of the fluid pressure gradient , which appears in them. Appropriate boundary and initial conditions are needed for the dependent variables listed above to solve the system of equations. For setting the initial conditions, the model is divided into two regions: the bed and the freeboard. For each of the regions specified above, boundary and initial conditions are specified.

2.3.1 Boundary Conditions

In this section the boundary conditions for the above governing equations, which relate to two dimensional fluidized bed with width "L" and height "H" to allow bed expansion typically i.e. the height of the bed is enough to prevent the particles throw out of the bed. Boundary conditions are imposed as follow:

$$x = 0 \;: v_g = v_s = u_g = u_s = 0, \quad \frac{\partial \varepsilon_g}{\partial x} = \frac{\partial T_g}{\partial x} = \frac{\partial T_s}{\partial x} = 0$$

$$x = \frac{L}{2} : \frac{\partial \varepsilon_g}{\partial x} = \frac{\partial T_g}{\partial x} = \frac{\partial T_s}{\partial x} = \frac{\partial v_g}{\partial x} = \frac{\partial u_g}{\partial x} = \frac{\partial v_s}{\partial x} = \frac{\partial u_s}{\partial x} = 0 \quad (symmetric)$$

$$y = 0 \;: v_g = V_{g,in}, \quad u_g = u_s = v_s = 0, \quad \varepsilon_g = 1, \quad P_g = P_{g,in}, \quad T_g = T_{g,in}, \quad \frac{\partial T_s}{\partial y} = 0$$

$$y = H : \frac{\partial v_g}{\partial y} = \frac{\partial u_g}{\partial y} = \frac{\partial T_g}{\partial y} = 0, \quad \varepsilon_g = 1, \quad v_s = u_s = 0, \quad P_g = P_{atm}$$

2.3.2 Initial Conditions

For setting the initial conditions, the model is divided into two regions: the bed and the freeboard. For each of the regions specified above, an initial condition is specified.

for bed region,

$$\varepsilon_g = \varepsilon_{g,mf}, \quad v_g = \frac{V_{g,mf}}{\varepsilon_{g,mf}}, \quad u_g = v_s = u_s = 0, \quad T_g = T_{g,in}, \quad T_s = T_{s,in}$$

for freeboard region,

$$\varepsilon_g = 1, \quad v_g = V_{g,mf}, \quad u_g = v_s = u_s = 0, \quad T_g = T_{g,in}$$

3. Methodology of Solution

The solution of the conservation equations was carried out using the finite difference technique. The method of solution used in the present work is described in details in this section. The details of this solution are given below:

1. Calculate the minimum fluidized velocity from the following equation [10]:

$$V_{g,mf} = 33.7\left[\left(1 + 3.59X10^{-5}\,Ar\right)^{0.5} - 1\right]\frac{\mu_g}{\left(d_p \rho_g\right)} \tag{35}$$

2. Calculate the gas void fraction at minimum fluidized velocity from the following equation [11]:

$$\in_{g,mf} = \frac{1}{2.1}\left[0.4 + \left(\frac{200\mu_g V_{g,mf}}{d_p^2(\rho_s - \rho_g)g}\right)^{1/3}\right] \tag{36}$$

3. Calculate the gas void fraction at entering gas velocity which given by:

$$\in_{g,in} = \frac{1}{2.1}[0.4 + (\frac{200\mu_g V_{g,in}}{d_p^2(\rho_s - \rho_g)g})^{1/3}] \tag{37}$$

4. Calculate the particle terminal velocity from the following equation [7]:

$$u_t = \left[-3.809 + \left(3.809^2 + 1.832Ar^{0.5}\right)^{0.5}\right]^2 \frac{\mu_g}{\rho_g d_p} \tag{38}$$

5. Specify stability of fluidized bed from the following equation [7]:

$$S = \frac{1.79}{n}\left(\frac{gd_p}{u_t^2}\right)^{0.5}\left(\frac{\rho_s - \rho_g}{\rho_s}\right)^{0.5}\left(\frac{\varepsilon_g^{1-n}}{(1-\varepsilon_g)^{0.5}}\right) - 1 \tag{39}$$

6. Determine the fluidized bed height at the entering velocity using the following equation [12] :

$$H1 = \frac{\left(1-\varepsilon_{g,mf}\right)}{\left(1-\varepsilon_{g,in}\right)} H_{mf} \tag{40}$$

7. Specify Initial and boundary conditions.
8. Call subroutine "cont" to solve particles phase continuity equations and evaluate the new time step particles volume fractions (ε_s^{n+1}) consequently evaluate (ε_g^{n+1}) from the equation (13).
9. Call subroutines "dirx" to solve momentum equation in x-direction and evaluate the new time step x-components velocities ($u_g^{n+1} and\ u_s^{n+1}$). In this subroutine, the following system of equations is solved to get values of x- component new step velocities ($u_g^{n+1} and\ u_s^{n+1}$).

$$\begin{pmatrix} A_{11} & A_{12} \\ (\varepsilon_s)_{i,j}^{n+1} & (\varepsilon_g)_{i,j}^{n+1} \end{pmatrix} \begin{pmatrix} (u_s)_{i,j}^{n+1} \\ (u_g)_{i,j}^{n+1} \end{pmatrix} = \begin{pmatrix} A_{13} \\ U_{gin} \end{pmatrix} \tag{41}$$

where:

$$A_{11} = \frac{\rho_s}{\Delta t} \tag{42}$$

$$A_{12} = \frac{\rho_g}{\Delta t} \tag{43}$$

$$\begin{aligned} A_{13} = {} & \frac{\rho_s}{\Delta t}(u_s)_{i,j}^n + \frac{\rho_g}{\Delta t}(u_g)_{i,j}^n - \frac{(u_s)_{i,j}^n}{\Delta x}\begin{cases} (u_s)_{i,j}^n - (u_s)_{i-1,j}^n & ,if\ (u_s)_{i,j}^n \geq 0.0 \\ (u_s)_{i+1,j}^n - (u_s)_{i,j}^n & ,if\ (u_s)_{i,j}^n < 0.0 \end{cases} \\ & - \frac{(v_s)_{i,j}^n}{\Delta y}\begin{cases} (u_s)_{i,j}^n - (u_s)_{i,j-1}^n & ,if\ (v_s)_{i,j}^n \geq 0.0 \\ (u_s)_{i,j+1}^n - (u_s)_{i,j}^n & ,if\ (v_s)_{i,j}^n < 0.0 \end{cases} - \frac{(u_g)_{i,j}^n}{\Delta x}\begin{cases} (u_g)_{i,j}^n - (u_g)_{i-1,j}^n & ,if\ (u_g)_{i,j}^n \geq 0.0 \\ (u_g)_{i+1,j}^n - (u_g)_{i,j}^n & ,if\ (u_g)_{i,j}^n < 0.0 \end{cases} \\ & - \frac{(v_g)_{i,j}^n}{\Delta y}\begin{cases} (u_g)_{i,j}^n - (u_g)_{i,j-1}^n & ,if\ (v_g)_{i,j}^n \geq 0.0 \\ (u_g)_{i,j+1}^n - (u_g)_{i,j}^n & ,if\ (v_g)_{i,j}^n < 0.0 \end{cases} \end{aligned} \tag{44}$$

10. Call subroutines "diry" to solve momentum equation in y-direction and evaluate the new time step y-components velocities ($v_g^{n+1} and\ v_s^{n+1}$).In this subroutine, the following system of equations is solved and used to get values of ($v_g^{n+1} and\ v_s^{n+1}$).

$$\begin{pmatrix} B_{11} & B_{12} \\ (\varepsilon_s)^{n+1}_{i,j} & (\varepsilon_g)^{n+1}_{i,j} \end{pmatrix} \begin{pmatrix} (v_s)^{n+1}_{i,j} \\ (v_g)^{n+1}_{i,j} \end{pmatrix} = \begin{pmatrix} B_{13} \\ V_{gin} \end{pmatrix} \tag{45}$$

where:

$$B_{11} = \frac{\rho_s}{\Delta t} + \beta\left(1 + \frac{(\varepsilon_s)^n_{i,j}}{(1-(\varepsilon_s)^n_{i,j})}\right) \tag{46}$$

$$\beta = C_d \frac{3(\varepsilon_s)^n_{i,j}\rho_g\left|(v_g)^n_{i,j} - (v_s)^n_{i,j}\right|}{4d_p}(1-(\varepsilon_s)^n_{i,j})^{-1.8} \tag{47}$$

$$B_{12} = -\frac{\rho_g}{\Delta t} - \beta\left(1 + \frac{(\varepsilon_s)^n_{i,j}}{(1-(\varepsilon_s)^n_{i,j})}\right) \tag{48}$$

$$\begin{aligned} B_{13} = {} & \frac{\rho_s}{\Delta t}(v_s)^n_{i,j} + \frac{\rho_g}{\Delta t}(v_g)^n_{i,j} - \frac{(u_s)^n_{i,j}}{\Delta x}\begin{cases} (v_s)^n_{i,j} - (v_s)^n_{i-1,j} & ,if\,(u_s)^n_{i,j} \geq 0.0 \\ (v_s)^n_{i+1,j} - (v_s)^n_{i,j} & ,if\,(u_s)^n_{i,j} < 0.0 \end{cases} \\ & - \frac{(v_s)^n_{i,j}}{\Delta y}\begin{cases} (v_s)^n_{i,j} - (v_s)^n_{i,j-1} & ,if\,(v_s)^n_{i,j} \geq 0.0 \\ (v_s)^n_{i,j+1} - (v_s)^n_{i,j} & ,if\,(v_s)^n_{i,j} < 0.0 \end{cases} - \frac{(u_g)^n_{i,j}}{\Delta x}\begin{cases} (v_g)^n_{i,j} - (v_g)^n_{i-1,j} & ,if\,(u_g)^n_{i,j} \geq 0.0 \\ (v_g)^n_{i+1,j} - (v_g)^n_{i,j} & ,if\,(u_g)^n_{i,j} < 0.0 \end{cases} \\ & - \frac{(v_g)^n_{i,j}}{\Delta y}\begin{cases} (v_g)^n_{i,j} - (v_g)^n_{i,j-1} & ,if\,(v_g)^n_{i,j} \geq 0.0 \\ (v_g)^n_{i,j+1} - (v_g)^n_{i,j} & ,if\,(v_g)^n_{i,j} < 0.0 \end{cases} - \frac{(\varepsilon_s)^n_{i,j} - (\varepsilon_s)^n_{i,j-1}}{dy}\left(3.2gd_p(\rho_s - \rho_g)\right) \end{aligned} \tag{49}$$

11. Call subroutine "temp" to solve energy equation and evaluate the new time step gas and solid particles temperatures ($T_g^{n+1} and\ T_s^{n+1}$).In this subroutine, the following system of equations is solved to get values of new time step temperatures for both phases ($T_g^{n+1} and\ T_s^{n+1}$).

$$\begin{pmatrix} C_{11} & C_{12} \\ D_{11} & D_{12} \end{pmatrix} \begin{pmatrix} (T_s)^{n+1}_{i,j} \\ (T_g)^{n+1}_{i,j} \end{pmatrix} = \begin{pmatrix} C_{13} \\ D_{13} \end{pmatrix} \tag{50}$$

where:

$$C_{11} = \frac{\rho_s C_{p,s}}{\Delta t}\left(\varepsilon_s^{n+1}\right) + (h_v)^{n+1}_{i,j} \tag{51}$$

$$C_{12} = (h_v)^{n+1}_{i,j} \tag{52}$$

$$\begin{aligned} C_{13} = {} & \frac{\rho_s C_{p,s}}{\Delta t}(\varepsilon_s T_s)^n_{i,j} - \frac{\rho_s C_{p,s}(u_s)^n_{i,j}}{\Delta x}\begin{cases} (\varepsilon_s T_s)^n_{i,j} - (\varepsilon_s T_s)^n_{i-1,j} & ,if\,(u_s)^n_{i,j} \geq 0.0 \\ (\varepsilon_s T_s)^n_{i+1,j} - (\varepsilon_s T_s)^n_{i,j} & ,if\,(u_s)^n_{i,j} < 0.0 \end{cases} \\ & - \frac{\rho_s C_{p,s}(v_s)^n_{i,j}}{\Delta y}\begin{cases} (\varepsilon_s T_s)^n_{i,j} - (\varepsilon_s T_s)^n_{i,j-1} & ,if\,(v_s)^n_{i,j} \geq 0.0 \\ (\varepsilon_s T_s)^n_{i,j+1} - (\varepsilon_s T_s)^n_{i,j} & ,if\,(v_s)^n_{i,j} < 0.0 \end{cases} + \frac{(\varepsilon_s K_s T_s)^n_{i+1,j} - 2(\varepsilon_s K_s T_s)^n_{i,j} + (\varepsilon_s K_s T_s)^n_{i-1,j}}{\Delta x^2} \\ & + \frac{(\varepsilon_s K_s T_s)^n_{i,j+1} - 2(\varepsilon_s K_s T_s)^n_{i,j} + (\varepsilon_s K_s T_s)^n_{i,j-1}}{\Delta y^2} + (\varepsilon_s \dot{q})^n_{i,j} \end{aligned} \tag{53}$$

$$D_{11} = (h_v)^{n+1}_{i,j} \tag{54}$$

$$D_{12} = \frac{\rho_g C_{p,g}}{\Delta t}\left(\varepsilon_g^{n+1}\right) + (h_v)^{n+1}_{i,j} \tag{55}$$

$$D_{13} = \rho_g C_{p,g} \frac{(\varepsilon_g T_g)^n_{i,j}}{\Delta t} - \frac{\rho_g C_{p,g} (u_g)^n_{i,j}}{\Delta x} \begin{cases} (\varepsilon_g T_g)^n_{i,j} - (\varepsilon_g T_g)^n_{i-1,j} & ,if\ (u_g)^n_{i,j} \geq 0. \\ (\varepsilon_g T_g)^n_{i+1,j} - (\varepsilon_g T_g)^n_{i,j} & ,if\ (u_g)^n_{i,j} < 0.0 \end{cases}$$
$$- \frac{\rho_s C_{p,g} (v_g)^n_{i,j}}{\Delta y} \begin{cases} (\varepsilon_g T_g)^n_{i,j} - (\varepsilon_g T_g)^n_{i,j-1} & ,if\ (v_g)^n_{i,j} \geq 0.0 \\ (\varepsilon_g T_g)^n_{i,j+1} - (\varepsilon_g T_g)^n_{i,j} & ,if\ (v_g)^n_{i,j} < 0.0 \end{cases} + \frac{(\varepsilon_g K_g T_g)^n_{i+1,j} - 2(\varepsilon_g K_g T_g)^n_{i,j} + (\varepsilon_g K_g T_g)^n_{i-1,j}}{\Delta x^2}$$
$$+ \frac{(\varepsilon_g K_g T_g)^n_{i,j+1} - 2(\varepsilon_g K_g T_g)^n_{i,j} + (\varepsilon_g K_g T_g)^n_{i,j-1}}{\Delta y^2} \tag{56}$$

12. Make gas residual check ,which given from the following equation :

$$d_g = (\varepsilon_g)^{n+1}_{i,j} - (\varepsilon_g)^n_{i,j} + \frac{\Delta t}{\Delta x} (u_g)^{n+1}_{i,j} \begin{cases} (\varepsilon_g)^{n+1}_{i,j} - (\varepsilon_g)^{n+1}_{i-1,j} & ,if\ (u_g)^{n+1}_{i,j} \geq 0.0 \\ (\varepsilon_g)^{n+1}_{i+1,j} - (\varepsilon_g)^{n+1}_{i,j} & ,if\ (u_g)^{n+1}_{i,j} < 0.0 \end{cases}$$
$$+ \frac{\Delta t}{\Delta y} (v_g)^{n+1}_{i,j} \begin{cases} (\varepsilon_g)^{n+1}_{i,j} - (\varepsilon_g)^{n+1}_{i,j-1} & ,if\ (v_g)^{n+1}_{i,j} \geq 0.0 \\ (\varepsilon_g)^{n+1}_{i,j+1} - (\varepsilon_g)^{n+1}_{i,j} & ,if\ (v_g)^{n+1}_{i,j} < 0.0 \end{cases} \tag{57}$$

- If $|d_g(i,j)| \leq \delta$ go to step 15, where δ is a small positive value here we let δ =5X10^{-3} .
- Else adjust ε_g^{n+1} by :

$$(\varepsilon_g)^{n+1}_{i,j} = (\varepsilon_g)^n_{i,j} - \frac{dt}{\Delta x} (u_g)^{n+1}_{i,j} \begin{cases} (\varepsilon_g)^{n+1}_{i,j} - (\varepsilon_g)^{n+1}_{i-1,j} & ,if\ (u_g)^{n+1}_{i,j} \geq 0.0 \\ (\varepsilon_g)^{n+1}_{i+1,j} - (\varepsilon_g)^{n+1}_{i,j} & ,if\ (u_g)^{n+1}_{i,j} < 0.0 \end{cases}$$
$$- \frac{\Delta t}{\Delta y} (v_g)^{n+1}_{i,j} \begin{cases} (\varepsilon_g)^{n+1}_{i,j} - (\varepsilon_g)^{n+1}_{i,j-1} & ,if\ (v_g)^{n+1}_{i,j} \geq 0.0 \\ (\varepsilon_g)^{n+1}_{i,j+1} - (\varepsilon_g)^{n+1}_{i,j} & ,if\ (v_g)^{n+1}_{i,j} < 0.0 \end{cases} \tag{58}$$

and calculate ε_s^{n+1} from equation (9).

13. Go to step 9 and calculate new time step velocities
14. Calculate the gas pressure values.
15. End program.

4. RESULTS AND DISCUSSION

The present hydrodynamic model is verified by comparing its results with MFIX code. The thermal model is tested and compared by available previous work experimental correlations. In this section the hydrodynamic and thermal results of present model is analyzed.

4.1 Hydrodynamic Results

Figure (2) shows the change of gas volume fraction at (0, 5, 10, 15 and 20 second) for sand particles of 400μm fluidized with air at velocity of 3 times minimum fluidized velocity. In the upper portion of Figure (2) the present work output data of variation of gas volume fraction with time are shown. While the lower portion shows the same variation at the same time for MFIX output data. It is clear that the bubbles traces and its directions are the same in the two figures. The positions of bubbles are slightly differ .

Figure (3) shows a comparison between the present model and MFIX code for gas volume fraction .Fair agreement between the present model results and MFIX output results for gas volume fraction variation with time is noticed.

The comparison of gas phase velocity for present model and MFIX is presented in Figures (4) and (5). Good agreement in direction and magnitude for two velocity component (u_g,v_g) is observed . It is noticed that u_g has a small value between (0.001 and 0.008 m/s) and its direction was changed, where v_g has a value between (0.23 to 0.65 m/s) and has the same upward direction.

Figures (6) and (7) show a comparison for the present model with MFIX for particle phase velocity. The two velocity component (u_s and v_s) are plotted against time variation from 0 to 20 seconds. The value of u_s is changed from0.006 m/s to 0.008 m/s with negative direction while the value of v_s changed from 0.08 m/s to 0.39 m/s and sometimes changes its direction.

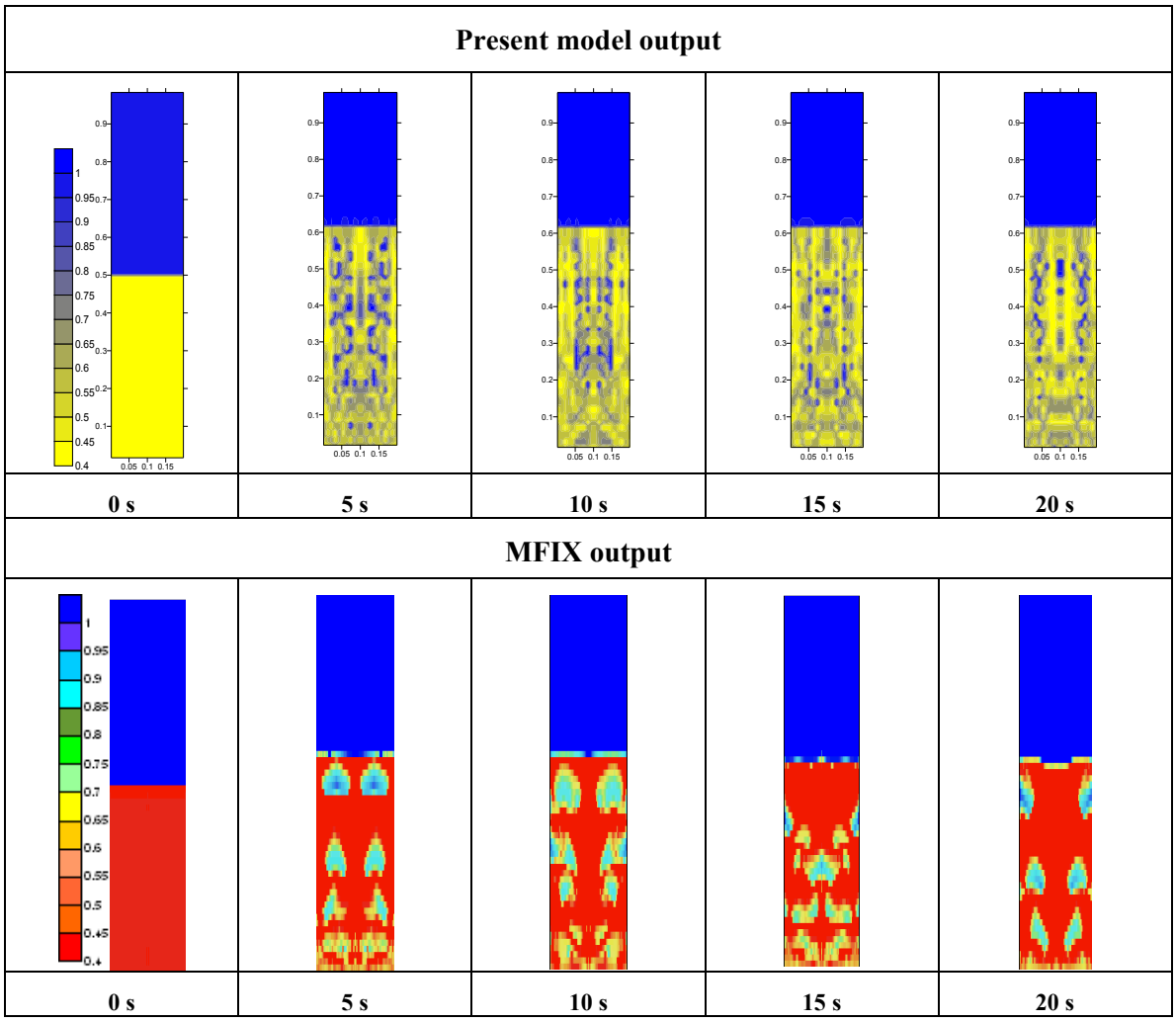

Figure (2): Variation of gas volume fraction for sand particles, d_p= 400µm ,$V_{g,in}$=3$V_{g,mf}$

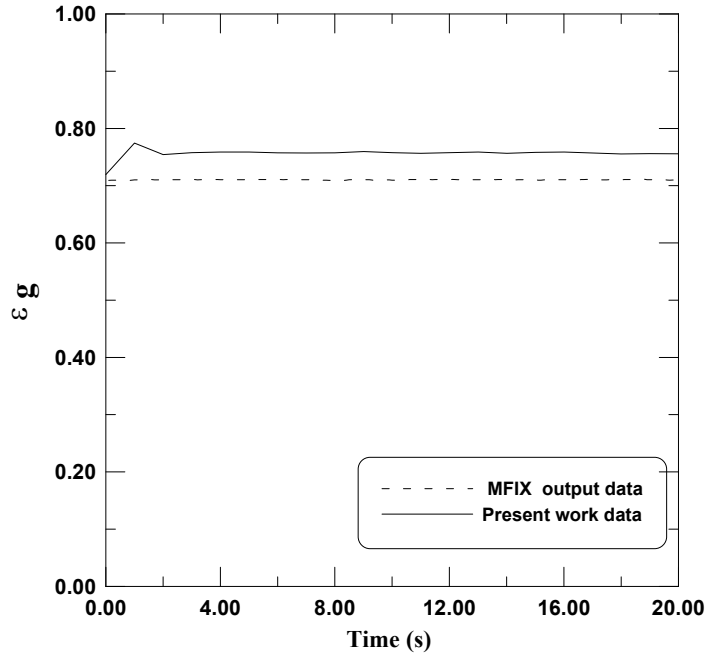

Figure (3): Comparison between MFIX and present model for gas volume fraction of sand particles, d_p= 400µm, $V_{g,in}=3V_{g,mf}$

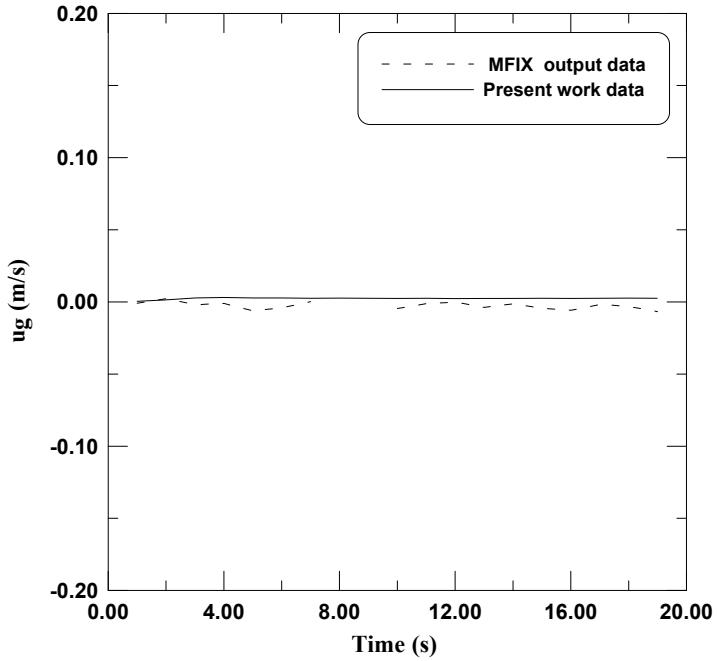

Figure (4): Comparison between MFIX and present model for gas phase velocity in x-direction of sand particles, d_p= 400µm ,$V_{g,in}=3V_{g,mf}$

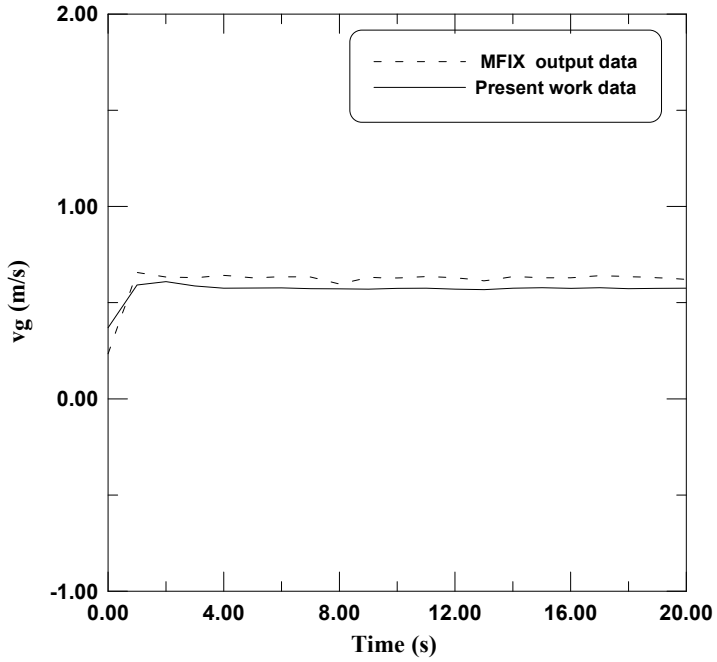

Figure (5): Comparison between MFIX and present model for gas phase velocity in y-direction of sand particles, d_p= 400µm ,$V_{g,in}$=3$V_{g,mf}$

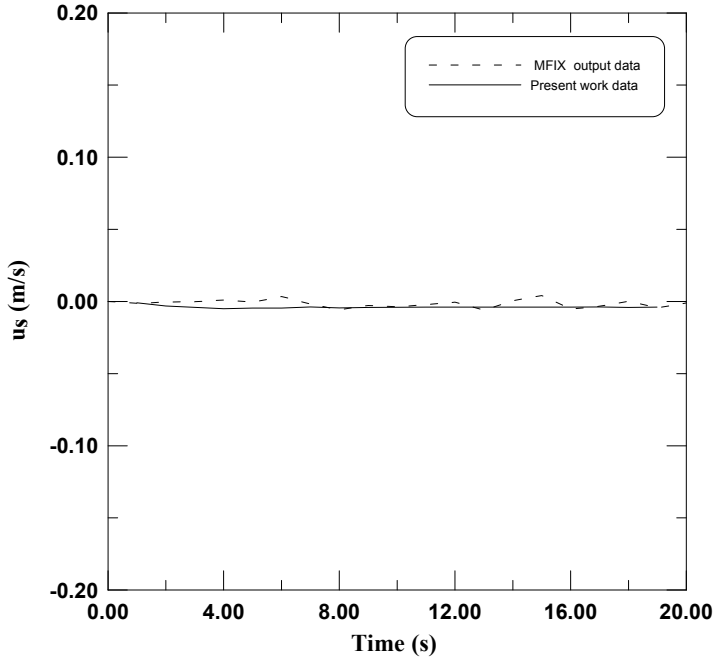

Figure (6): Comparison between MFIX and present model for particle phase velocity in x-direction of sand particles, d_p= 400µm ,$V_{g,in}$=3$V_{g,mf}$

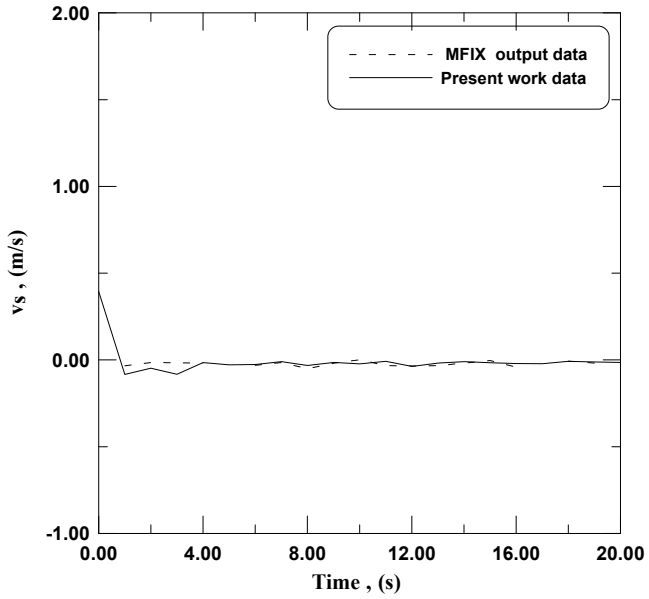

Figure (7): Comparison between MFIX and present model for particle phase velocity in y-direction of sand particles, d_p= 400µm ,$V_{g,in}$=3$V_{g,mf}$

The gas pressure fluctuation in the bed and in the free board regions are presented in figure(8). The figure is presented for sand particles of 400µm fluidized with air at velocity of 3 times minimum fluidized velocity at time period 20 seconds. Also the comparison between the present model and MFIX data are shown in this figure. As it is known the total pressure drop across the bed is constant after reached the minimum fluidization velocity. For both present model and MFIX, the gas pressure is changed from 108415 Pa at the bottom of the bed to 101325 Pa at the top of the bed. It is noticed that present model gas pressure are higher than the MFIX data in the bed region and a small part of freeboard region .This is due to the variation of the fluidization head between the two models. Although there is a little difference between the two models but the trend of the two curves are the same.

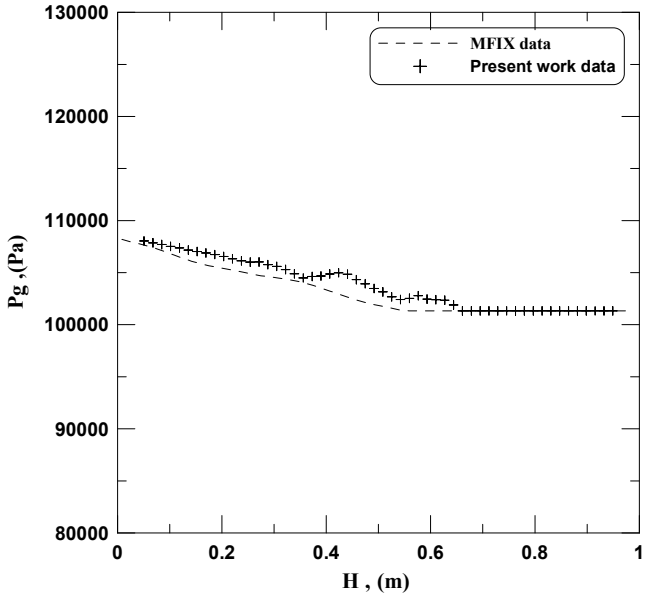

Figure(8): Comparison between MFIX and present model for gas pressure after 20 seconds (sand particles) , d_p= 400µm ,$V_{g,in}$=3$V_{g,mf}$

The continuity equation for the gas phase is used to check the hydrodynamic model by constitute a gas residual term d_g. This term is actually is near zero but the present model limits it by 5×10^{-3} for its absolute value to deal easy with the computer calculations and overcome floating errors. Figure (9) shows that the absolute value of d_g for sand particles of 400μm fluidized with air at velocity of 3 times minimum fluidized velocity at time period 20 seconds is not exceed 3×10^{-3} . This is an indication for the accuracy of the calculations of the present model .

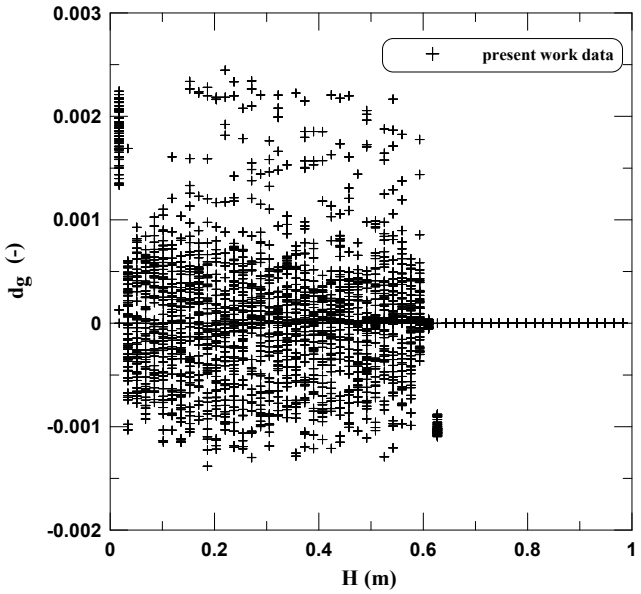

Figure (9): Gas residual check for sand particles at 20 seconds, d_p= 400μm ,$V_{g,in}$=3$V_{g,mf}$

In this section the input gas velocity is changed from one to nine times minimum fluidized velocity for 500 μm sand particles to study the the effect of this parameter on fluidization behavior. Input gas velocity has an effective role in thermal performance of the fluidized bed. In order to illustrate its effect, the relation between Nusselt number and flow number is described in Figure (10). It is clear from this figure that with increase in flow numbers, the Nusselt number increases until reached an optimum flow number where the Nusselt number reaches its maximum value. After this optimum value the increase in flow number is associated with a decrease in Nusselt number. This decrease in Nusselt number may be due to the increase of input gas velocity toward the terminal velocity, consequently the bed goes to be empty bed.

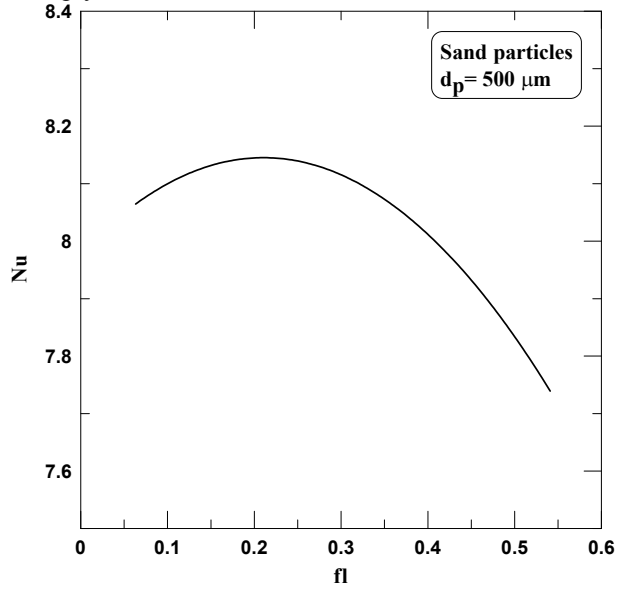

Figure (10): Variation of Nusselt number with flow number

4.2 Thermal Results

The relation between the average heat transfer coefficient in fluidized bed and the particle diameter are one of the characterization curves of fluidized bed. Figure (11) gives an indication of the range of average heat transfer coefficient of the bed and effect of particle diameter [13].

So, the present work results for sand particles with particles diameter 100, 200, 300, 400, 500, 600, 700, 800, 900 and 1000 μm with input gas velocity three times of minimum fluidized velocity are presented in Figure (11). The comparison of heat transfer coefficient of the present model data and that of reference [13] shows the good agreement of present model with this reference.

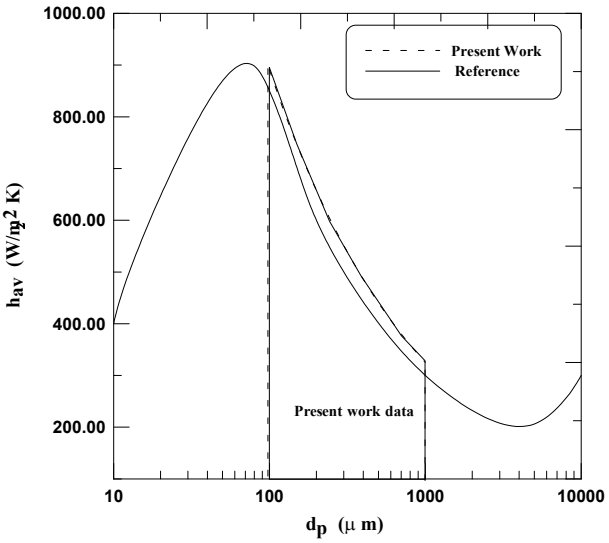

Figure (11): Comparison of the present model result and results of Botterill [12]

As it is known the plotting of Nusselt number against Reynolds number gives a good presentation of the strong of the thermal behavior as highest Nusselt number is an indicator of highest heat transfer coefficient. Reynolds number for present model for sand particles of diameters 100, 200, 300, 400, 500, 600, 700, 800, 900 and 1000 μm and fluidized with air at three times minimum fluidized velocity is in range from 0.3 to115. Figure(12) shows the relation between Nusselt and Reynolds number for present model. This relation is compared with these of ZENZ [2] and Gunn [3]. It is clear that the present model lies slightly higher than the two equations and is in good agreement with them.

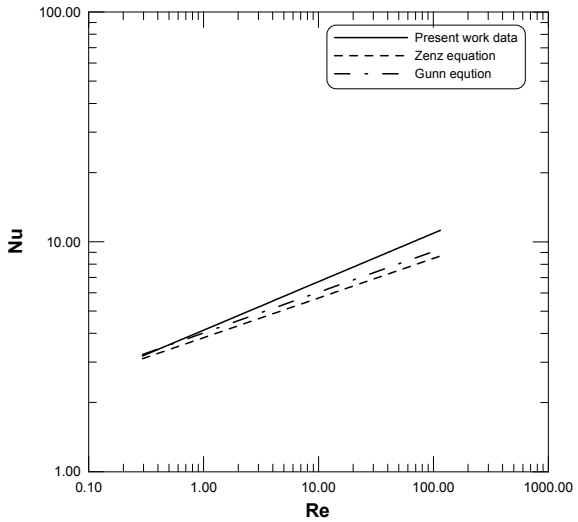

Figure (12): Comparison between present model, Zenz equation and Gunn equation

5. CONCLUSION

The present work creates a mathematical modeling and numerical simulation of the hydrodynamics and heat transfer processes in a gas fluidized bed with a vertical uniform gas velocity at the inlet. The velocity, volume fraction, gas pressure, temperature distribution and heat transfer coefficient are studied. The results of the modelling and simulation may be briefly summarized as:

1. The present work hydrodynamic model results are in good agreement with MFIX results
2. The thermal model of the present work confirms Zenz and Gunn equations.
3. The present work model can be used for simulation of uniform fluidization and give good results.
4. The present model describes the hydrodynamic and thermal behavior of fluidized bed.
5. The average Nusselt number increases with the increase of flow number until reached to optimum flow number. After reached optimum flow number the Nusselt number begins to decrease. The optimum flow number presents the optimum input gas velocity which enters the fluidized bed system.

NOTATION

Ar	Archimedes number, $Ar = \frac{g d_p^3 \rho_g (\rho_s - \rho_g)}{\mu_g^2}$	
C_d	Drag coefficient, $C_d = \left(0.63 + \frac{4.8}{\mathrm{Re}^{0.5}}\right)^2$	
$C_{p,g}$	Specific heat of fluidizing gas at constant pressure	J/kg.K
$C_{p,s}$	Specific heat of solid particles	J/kg.K
d_g	Residue of the gas continuity equation	Kg/m^3 s
d_p	Mean particle diameter	m
g	Acceleration due to gravity	m/s^2
F_{gx}	Total gas phase force in x direction per unit volume	N /m^3
F_{gy}	Total gas phase force in y direction per unit volume	N /m^3
F_{sx}	Total particle phase force in x direction per unit volume	N /m^3
F_{sy}	Total particle phase force in y direction per unit volume	N /m^3
fl	Flow number , $fl = \frac{V_{g,in}}{u_t}$	
h_{gp}	Heat transfer coefficient between gas phase and particle phase	W/m^2.K
h_v	Volumetric heat transfer coefficient , $h_v = \frac{6(1-\varepsilon_g)h_{gp}}{d_p}$	W/m^3.K
H	Total height of the bed and freeboard	m
H_{mf}	Minimum fluidized head of the bed	m
H1	Expansion head of bed at the input velocity	m
k_g	Thermal conductivity of gas phase	W/m.K
k_s	Thermal conductivity of particle phase	W/m.K
L	Width of the bed	m
Nu	Nusselt number based on particle diameter, ($Nu= h_{gp}d_p/k_g$)	
P_g	Gas pressure	Pa
Pr	Prandtl number , $Pr= \mu_g C_{pg}/k_g$	
$\dot{q}$	Rate of heat generated with in particle phase	W/m^3
u_g	Gas phase velocity in x direction	m/s
U_{gin}	Input gas velocity to the bed in x direction	m/s
u_s	Particle phase velocity in x direction	m/s
u_t	Particle terminal velocity	m/s
U_r	Relative velocity between two phases	m/s
Re	Reynolds number, $\mathrm{Re} = \frac{\varepsilon_g \rho_g d_p \lvert\overrightarrow{U_r}\rvert}{\mu_g}$	

S	Stability function	
t	Time	s
T_g	Gas phase temperature	C°
T_s	Particle phase temperature	C°
TFM	Two fluid model	
v_g	gas phase velocity in y direction	m/s
$V_{g,mf}$	Gas minimum fluidized velocity	m/s
$V_{g,in}$	Input gas velocity to the bed in y direction	m/s
v_s	Particle phase velocity in y direction	m/s

Greek Letters

ΔP_B	Total Pressure drop across the bed	Pa
Δt	Time step	s
Δx	Length of cell in the computational grid	m
Δy	height of cell in the computational grid	m
ϵ_g	Gas phase volume fraction	
$\epsilon_{g,mf}$	Gas phase volume fraction at minimum fluidization	
ϵ_{in}	Gas volume fraction at the input velocity	
ϵ_s	Particle phase volume fraction	
ρ_g	Density of gas phase	Kg/m^3
ρ_s	Density of particle phase	Kg/m^3
ρ_{sus}	Suspension density	Kg/m^3
μ_g	Viscosity of gas	Pa.s
δ	Small positive value = $5X10^{-3}$	

REFERENCES

[1] Madhava Syamlal, "MFIX Documentation User's Manual", U.S. Department of Energy, Office of Fossil Energy, Morgantown Energy Technology Center, USA (2006).

[2] F.A., Zenz, "State of the Art Review and report on Critical Aspects and Scale-Up Considerations in the Design of Fluidized Bed Reactors", 1983.

[3] H. Enwald and E. Peirano," Gemini: A Cartesian Multiblock Finite Difference", Code for Simulation of Gas-Particle Flows", Department of Thermo and Fluid Dynamics, Chalmers University of Technology, No. 412 96, Goteborg, Sweden (1997).

[4] C. Torres and E. Ananay, "Modelling of Circulating Fluidized Bed using Computational Fluid Dynamic Software", M.Sc. Thesis, Mechanical Department, Faculty of Engineering, University of New Brunswick , Canada (2000).

[5] C.C. Pain, S. Mansoorzadeh, J.L.M. Gomes, C.R.E. de Oliveira , "A Numerical Investigation of Bubbling Gas–Solid Fluidized Bed Dynamics in 2-D Geometries", Powder technology , Vol. 128 ,pp. 56–77, 2002.

[6] Paola Lettieri, Luca CammarataGiorgi, D. M. Micale and John Yates, " CFD Simulations of Gas Fluidizd Beds Using Alternative Eulerian–Eulerian Modelling Approaches ",International Journal Of Chemical Reactor Engineering, Article 5 , Vol. 1,2003 .

[7] L.G. Gibilaro, "Fluidization Dynamics", Butter Worth-Heinemann, Oxford (2001).

[8] Max Savransky," Numerical Simulations of Thermo-Fluid Phenomena in Microwave Heated Packed and Fluidized Beds" ,Ph.D. thesis, Faculty of the Virginia Polytechnic Institute and State University, USA, 2003.

[9] J. Kodikal, Nilesh Kodikal and H. Bhavnani Sushil , Paper No. FBC99-0077, "Proceedings of the 15th International Conference on Fluidized Bed Combustion", May 16-19, Savannah, Georgia (1999).

[10] D. Kunii and O. Levenspiel, "Fluidization Engineering", John Wiley & sons, New-York (1969).

[11] A. Kumar, "Design, Construction, and Operation of 30.5 cm Square Fluidized Bed for Heat Transfer Study", Master of Technology, Indian Institute of Technology, Madras, India (1986).

[12] M. Rhodes, "Introduction to Particle Technology", John Wiley & sons, London (1998).

[13] J.S.M. Botterill, "Fluid Bed Heat Transfer", Academic press, London (1975).